Applied Numerical Modeling in Geomechanics – 2020 – Billaux, Hazzard, Nelson & Schöpfer (eds.) Paper: 09-02

3DEC analysis of crosswise tension resistance in masonry structures

Shipeng Chen & Katalin Bagi
Department of Structural Mechanics, Budapest University of Technology and Economics, Budapest, Hungary

1 INTRODUCTION

Previous research works (Simon & Bagi 2014, Beatini et al. 2018) pointed out that masonry shells with no-tension joints can exhibit considerable resistance to hoop (i.e. horizontal) tension because of the frictional forces arising in the horizontal joints due to meridional (i.e. vertical) compression, and this phenomenon can give a considerable extra resistance to the structures. The aim of our study was to predict this hoop-directional tension resistance in case of different bond patterns, and to check the validity of the theoretical predictions with the help of *3DEC* (Itasca 2013) discrete element simulations. Simple running bond, Flemish bond and herringbone patterns (Fig. 1, top row) were investigated in our study.

The complete analysis of each bond pattern consisted of the following three steps: (1) based on the statics of a suitably chosen elementary cell, theoretical prediction was derived to the magnitude of the hoop tension resistance in terms of the magnitude of meridional compression and the contact friction coefficient; (2) the same elementary cell was simulated with *3DEC* and the prediction is checked; (3) the results were validated using a large structural model, i.e. a cylindrical shell submitted to vertical compression and a gradually increasing outwards surface pressure on the internal surface of the cylinder which results in hoop tension.

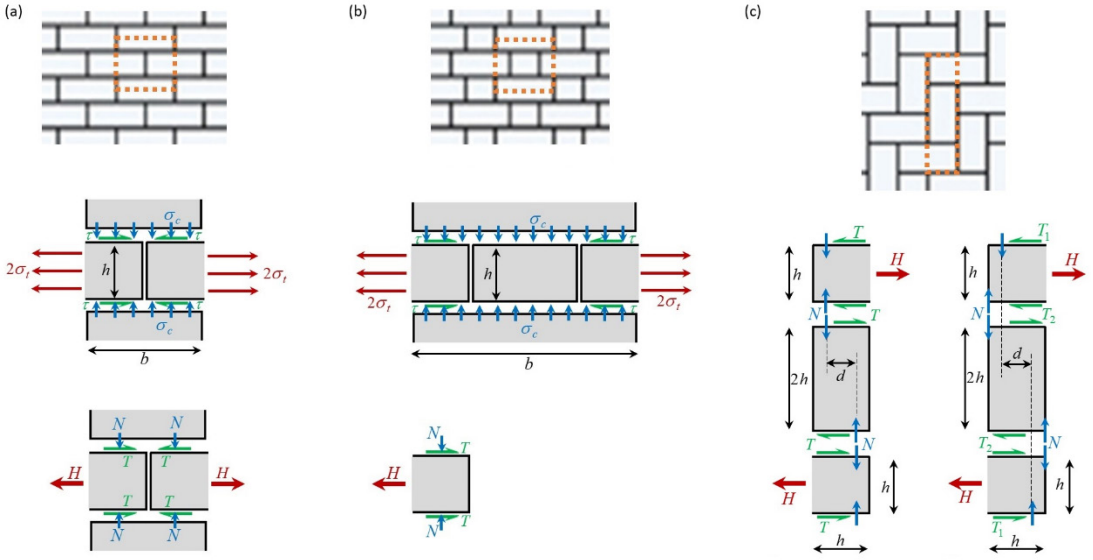

Figure 1. (a) running bond pattern, (b) Flemish bond pattern, (c) herringbone pattern.

2 THEORETICAL DERIVATIONS

2.1 *The running bond pattern*

Figure 1a presents that elementary cell of a wall with simple running bond pattern whose equilibrium analysis at the initiation of sliding failure serves as the basis for finding the relation between the horizontal average tension stress, σ_t , and the vertical average compression stress on the horizontal surface, σ_c. The τ shear stress on the horizontal surfaces cannot exceed the friction limit, i.e. $\mu \cdot \sigma_c$, where μ is the friction coefficient. The length of the bricks is b, their height is h, and their thickness perpendicular to the plane of the wall is t.

The horizontal equilibrium equation of one of the two truncated blocks in the middle is $H = 2\ T$; or equivalently, $2\sigma_t \cdot h \cdot t = 2\ \tau \cdot (b/2) \cdot t$:

$$\left(2\sigma_t\right) \cdot h \le 2\left(\mu \cdot \sigma_c\right) \cdot \frac{b}{2} \tag{1}$$

from which (taking into account that $\tau = \mu \cdot \sigma_c$ at failure) the following theoretical prediction is received for the hoop tension resistance:

$$\sigma_t \le \mu \frac{b}{2h} \cdot \sigma_c \tag{2}$$

2.2 *The Flemish bond pattern*

Similar derivations can be done for the Flemish bond pattern (Figure 1b). Note that in case of a Flemish pattern, the thickness of the wall is twice as much as in case of a running bond pattern wall constructed of the same size of bricks, and the perpendicularly placed bricks of the Flemish wall (middle block in Figure 1b) do not take part in carrying the crosswise tension. The result turns out to be similar:

$$\sigma_t \le \mu \frac{b}{4h} \cdot \sigma_c \tag{3}$$

2.3 *The herringbone pattern*

In herringbone pattern the vertical bricks are endangered for tipping over and, corresponding to whether such a motion takes part in the failure or not, two kinds of failure modes can occur. For unrealistically low frictional resistance (i.e. $\mu \le 0{,}5$) the vertical bricks do not rotate, and the failure is due to pure sliding: the contact shear stress resultant T reaches the friction limit on all surfaces. This failure mode is shown in Figure 1c, bottom left. (In this case the distance d of the normal resultants N is equal to what is needed to keep the moment balance of the vertical brick: $d \cdot N = 2h \cdot T$.) The hoop tension resistance turns out to be

$$\sigma_t \le \frac{1}{2} \mu \cdot \sigma_c \tag{4}$$

For larger, i.e. more realistic friction coefficient ($\mu \le 0{,}5$ and above) the limitation for hoop tension resistance becomes affected by the moment balance of the vertical bricks (Fig. 1c, bottom right). From the moment equation of the vertical bricks, from the horizontal force balance of the truncated horizontal bricks, and from the moment balance of the whole elementary cell, the following hoop tension resistance is derived:

$$\sigma_t \le \frac{0{,}5 + \mu}{4} \cdot \sigma_c \tag{5}$$

3 *3DEC* SIMULATIONS

The discrete element simulations were done on two types of models: elementary cells of planar walls, and on cylindrical shells. In every test, a vertical compression load was first expressed on the structure (self-weight was neglected). Then a gradually increasing horizontal tension was given, until further increase

could not be resisted any more (i.e. the equilibrium could not be found for this state). The horizontal stresses were increased in 50 N/m^2 steps, and the highest equilibrated tension stress magnitude was detected and considered the as crosswise tension resistance.

The material parameters imitated a brick structure consisting of deformable elements with dry (frictional) contacts. According to the experimental calibration tests by Fódi (2011), the following material characteristics were used. The data for the elements: density 1428 kg/m^3, bulk modulus: $1.10 \cdot 10^{10}$ N/m^2, shear modulus $0.833 \cdot 10^{10}$ N/m^2. The characteristics of the joints: normal contact stiffness $1.0 \cdot 10^{10}$ $(N/m^2)/m$, shear contact stiffness $0.70 \cdot 10^{10}$ $(N/m^2)/m$, friction angle 38°.

The bricks were of 0.25 m × 0,065 m × 0.125 m size: for the running and herringbone patterns the 0.125 m was the perpendicular dimension (so in the plane of the analysis the length-to-height ratio was 4:1); while in case of the Flemish pattern the perpendicular size was 0.25 m = 2 × 0.125 m.

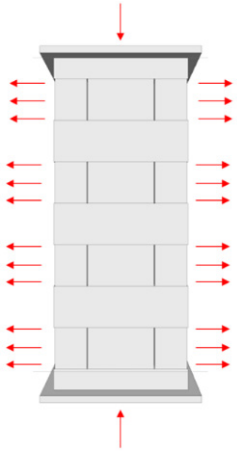

Figure 2. The structure considered in the convergence analysis.

3.1 *Convergence analysis*

3DEC considers the deformability of the discrete elements in such a way that the elements are subdivided into uniform-strain tetrahedral finite elements. In order to get realistic information on how the structures behave, first the necessary density of the applied uniform-strain tetrahedral mesh had to be determined. This was done with the help of the structure shown in Figure 2 having 0.25 m width, 8 × 0.065 m total height between the top and bottom loading plateau, and 0.25 m thickness perpendicular to the plane of Figure 2. This structure was loaded vertically by 4167 N/m^2 compression, and then submitted to a gradually increasing horizontal tension. The simulation was repeated by using different densities for the tetrahedral subdivision inside the discrete elements.

Table 1 shows that with increasing subdivision density, the failure tension stress converged to a specific value, which was approximated with about 2% accuracy by the rough meshing and with better than 1% accuracy by the medium meshing. We concluded that the medium meshing is sufficient for further analysis wherever the crosswise tension resistance is to be determined.

Table 1. Convergence analysis on the necessary density of tetrahedral meshing.

	Mesh size (m)	Computation time (min)	Limit tensile stress (N/m^2)	Deviation from "Very dense meshing"
Rough meshing	0.03	8	5830	1,9 %
Medium meshing	0.02	16	5760	0,7 %
Dense meshing	0.01	171	5730	0,2 %
Very dense meshing	0.005	2838	5720	---

3.2 *Simulation results on the elementary cells*

The diagrams in Figure 3 summarize the results of the *3DEC* simulations done on the elementary cells on which the theoretical predictions were derived. The horizontal axis shows the applied vertical compression stress; the vertical axis measures the crosswise tension resistance as a function of the vertical compression. The theoretical predictions are shown in solid lines and the simulation results are marked by the dots. The dependence is clearly linear, and the simulation results strongly coincide with the theoretical predictions.

3.3 *Validation of the results: Cylindrical shells*

The above theoretical predictions are being checked with the help of vertically standing cylindrical shells, submitted to vertical compression and then to increasing outwards loading that produces horizontal hoop tension. The presentation will introduce the results of these validation tests.

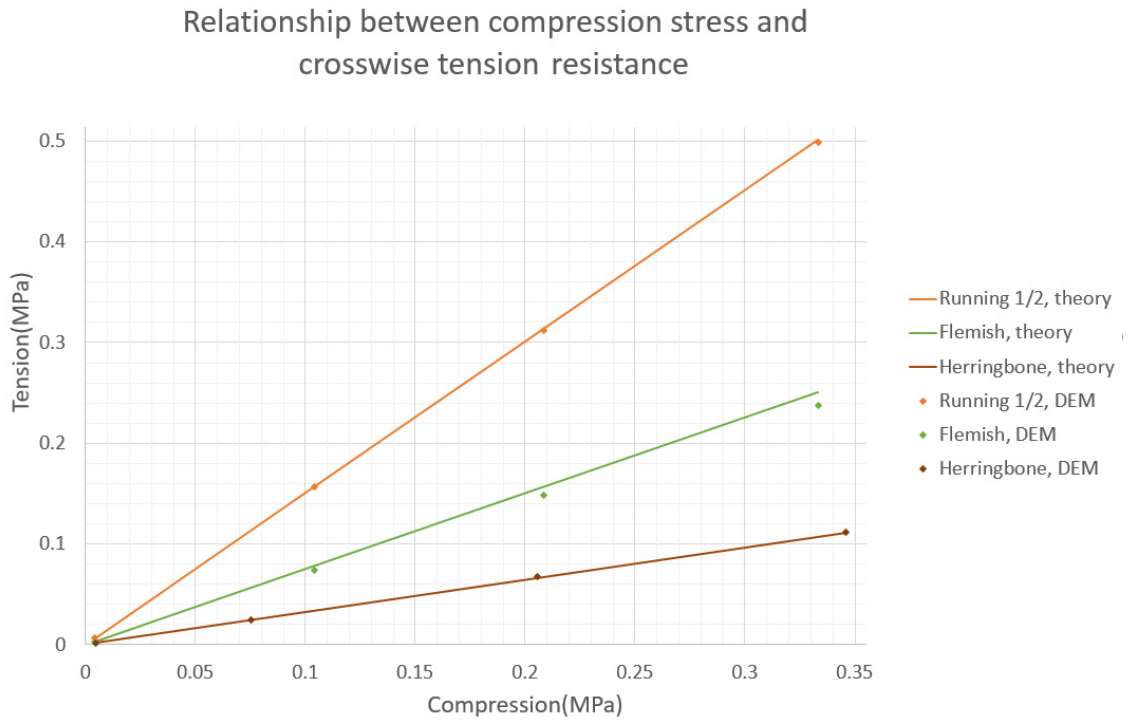

Figure 3. Failure tension stress for the different bond patterns.

4 CONCLUSIONS AND FUTURE RESEARCH

The hoop tension resistance due to the friction in the horizontal joints for three different bond patterns were derived, and then checked with *3DEC* simulations. In case of the herringbone pattern two different failure modes were identified, depending on the magnitude of the contact friction resistance: a purely sliding mode, and a combined tipping-over-and-sliding mode.

The results for the crosswise tension resistance can be applied for the analysis of masonry shells (e.g. spherical domes and fan vaults) where the traditional calculations assume zero hoop tension resistance. With formulas (2)-(5) the extra load bearing capacity of these shells can be quantified and taken into consideration by the structural engineer.

REFERENCES

Beatini, V., Royer-Carfagni, G. & Tasora, A. 2018. The role of frictional contact of constituent blocks on the stability of masonry domes. *Proc. R. Soc. A* 474: 20170740.

Fódi, A. 2011. *Experimental and numerical investigation of reinforced and plain masonry walls*. PhD Dissertation, Budapest University of Technology and Economics, Budapest, Hungary.

Itasca Consulting Group, Inc. 2013. *3DEC – Three-Dimensional Distinct Element Code, Ver. 5.2 User's Manual*. Minneapolis: Itasca.

Simon, J. & Bagi, K. 2014. Discrete element analysis of the minimum thickness of oval masonry domes. *International Journal of Architectural Heritage* 10: 457-475.